4. Rosenblueth, E. *Proc. 2nd World Conf. Earthquake Engng*, Japan, 1 (1960).
5. Bustamante, J. I. & Rosenblueth, E. *Proc. 2nd World Conf. Earthquake Engng*, Japan, 2, 879–894 (1960).
6. Scawthorn, C., Iemura, H. & Yamada, Y. *Earthquake Engng struct. Dynam.* **9**, 93–115 (1981).
7. Booth, E. *New civ. Engr.* 16–17 (4 April 1985).
8. Tezcan, S. S., Yerlici, V. & Durgunoglu, H. T. *Earthquake Engng struct. Dynam.* **6**(4), 397–421 (1978).
9. Berg, G. V., Bolt, B. A., Sozen, M. A. & Rojahn, C. *Earthquake in Romania 4 March 1977: An Engineering Rep.* (National Academy Press, Washington DC, 1980).
10. Tezcan, S. S. & Ipek, M. *Earthquake Engng struct. Dynam.* **1**, 203–215 (1973).
11. Berg, G. V. *The Skopje, Yugoslavia Earthquake 26 July 1963* (American Iron and Steel Institute, New York, 1964).
12. Newmark, N. M., Blume, J. A. & Kapur, K. K. *J. Pwr Div. Am. Soc. Civ. Engrs* **99**, No. PO2, 287–303 (1973).
13. Berg, G. V. *Seismic Design Codes and Procedures* (Earthquake Engineering Research Institute, Berkeley, California, 1982).
14. Dowrick, D. J. *Earthquake Resistant Design* (Wiley, London, 1977).
15. Rosenblueth, E. *Design of Earthquake-resistant Structures* (Pentech, London, 1980).
16. *Seismic Design for Buildings*, TM-5-809-10, 23-26 (US Departments of Army, Navy and Air Force, Washington, DC, 1973).
17. Douglas, B. M. & Trabert, T. E. *Bull. seism. Soc. Am.* **63**(3), 1025–1039 (1973).
18. Hart, G. C., Di Julio, R. M. & Lew, M. *J. struct. Div. Am. Soc. civ. Engrs* **101**, No. ST2, 397–416 (1975).
19. Jennings, P. C., Matthiesen, R. B. & Hoerner, J. B. *Earthquake Engng struct. Dynam.* **1**(2), 107–132 (1972).
20. Newmark, N. M. *Proc. 4th World Conf. Earthquake Engng*, Santiago, Chile, 2, Pt A3, 19–32 (1969).
21. *Earthquake Resistant Regulations, A World List* (International Association for Earthquake Engineering, Tokyo, 1984).
22. Chandler, A. M. thesis, Univ. London (1985).
23. Wilson, E. L. & Dovey, H. H. *Static and Earthquake Analysis of Three-dimensional Frame and Shear Wall Buildings—TABS* University of California, Berkeley Rep. EERC 72-01 (1972, revised 1977).
24. Wilson, E. L. *et al. Extended Three-dimensional Analysis of Building Systems-ETABS* University of California, Berkeley Rep. EERC 75-13 (1975).
25. Ayre, R. S. *Bull. seism. Soc. Am.* **33**(2), 91–119 (1943).
26. Housner, G. W. & Outinen, H. *Bull. seism. Soc. Am.* **48**(2), 221–229 (1958).
27. Kan, C. L. & Chopra, A. K. *J. struct. Div. Am. Soc. civ. Engrs* **103**, No. ST4, 805–819 (1977).
28. Rosenblueth, E. & Elorduy, J. *Proc. 4th World Conf. Earthquake Engng*, Santiago, Chile, 1, Pt A1, 185–196 (1969).
29. Dempsey, K. M. & Irvine, H. M. *Earthquake Engng struct. Dynam.* **7**(2), 161–180 (1979).
30. Tsicnias, T. G. & Hutchinson, G. L. *Proc. Instn civ. Engrs* **71**, 821–843 (1981).
31. Kan, C. L. & Chopra, A. K. *Earthquake Engng struct. Dynam.* **5**(4), 395–412 (1977).
32. Gluck, J., Reinhorn, A. & Rutenberg, A. *Proc. Instn civ. Engrs* **67**, 411–424 (1979).
33. Hall, J. F. *Earthquake Engng struct. Dynam.* **10**, 797–811 (1982).
34. Rosenblueth, E. *Earthquake Engng struct. Dynam.* **7**(1), 49–61 (1979).
35. Winney, M. *et al. New civ. Eng.* 4–5 (26 September 1985).
36. Berg, G. V. & Hanson, R. D. *Proc. 5th World Conf. Earthquake Engng*, Rome, Session 1A (1973).

ARTICLES

DNA bending at adenine·thymine tracts

Hyeon-Sook Koo, Hen-Ming Wu & Donald M. Crothers

Department of Chemistry, Yale University, New Haven, Connecticut 06511, USA

Intrinsic bending of DNA molecules results from local structural polymorphism in regions of homopolymeric dA·dT which are at least 4 base pairs long; the A·T tracts must be repeated in phase with the helix screw. Bending, in the direction of base-pair tilt rather than roll, occurs at the junctions between the A·T tract and adjacent B-DNA, with a larger angle at the 3′ than at the 5′ end of the A tract.

SEQUENCE-directed bending of the DNA helix is now generally thought to be the origin of the anomalously slow gel electrophoretic mobility of DNA fragments isolated from the kinetoplast body of tropical parasites[1–7], and from other sources such as the origin of replication of bacteriophage λ (ref. 8). Wu and Crothers[6] used the variation in gel mobility to map a bending locus contained in a *Sau*3A restriction fragment isolated from *Leishmania tarentolae* kinetoplast DNA, and identified the sequence

–GAATTCCCAAAAATGTCAAAAAATAGGCAAAAAATGCCAAAAATCCCAAAC–
↑
bend centre

at the bending locus. The striking feature observed is a regular repeat of the sequence element $CA_{5-6}T$ with 10-base pair (bp) periodicity around the centre of the bend. Presumably each A_n tract produces a small bend in the DNA helix axis; repetition of these elements in phase with the helix screw results in their coherent addition to form a large overall bend. The objective of the work reported here is to explore this model, including the predicted role of phasing, the possible importance of increased helix flexibility, the strictness of the requirement for a continuous run of A residues, and the potential role of the junctions with other bases flanking the A tracts.

We approached the problem by chemical synthesis of appropriate oligonucleotides (Table 1) and their complementary strands, adjusted so that the resulting duplexes contained single-stranded regions at the ends which allowed ligation in a unique polarity to form longer DNA molecules containing up to 30 repeats of the oligonucleotide. Gel mobility anomalies in the multimers were assayed by running the ligation products on polyacrylamide gels, with ligated 10-bp *Bam*HI linkers as size standards. It is expected that increased bending, with the accompanying decrease in DNA end-to-end distance, should lead to decreased gel-electrophoretic mobility[9,10]. We define the apparent length of each multimer as being equal to the length of the marker DNA having the same mobility; the experimentally determined ratio R_L of apparent length to real length is assumed to be an increasing function of the extent of bending.

Influence of phasing

The role of phasing of the bending loci was addressed by examining a set of sequences $(A_5N_k)_n$ ($k = 4, 5, 6, 7, 10$), each of which contains the tract A_5, flanked 3′ and 5′ by C, with a total of k bases intervening in the G+C-rich segment between the A_5 tracts. As shown in Figs 1 and 2, the gel mobility is strongly affected by the phasing of the A_5 tracts. Minimum mobility is seen for the series $(A_5N_5)_n$ in which the 10-bp phasing nearly matches the expected helix screw of about 10.3 bp per turn, calculated from the average of 10.5 for B-DNA and 10.1 for poly(dA)·poly(dT) in solution[11–13]. A substantial but smaller anomaly in electrophoretic mobility is seen for the series $(A_5N_6)_n$, while $(A_5N_4)_n$ and $(A_5N_7)_n$ behave more normally. Hence, the results confirm the prediction that bending elements must be repeated in phase with the helix screw in order to add coherently.

The normal gel mobility of the series $(A_5N_{10})_n$ is important for distinguishing between bending due to increased flexibility and systematic bending in which the direction of the helix axis is altered in a definite way. Suppose, for example, that A_n tracts have increased flexibility because of relatively easier bending by roll into the major and minor grooves. Such bending is predominantly in a fixed plane, so the effects should sum coherently if the A_n units are separated by either an integral or a half-integral number of turns. Since the experiments show no bending when the separation is half-integral, we conclude that the bends have directional preference, and the series $(A_5N_{10})_n$ has normal mobility because it forms a zig-zag structure in which

the systematic bends are nearly exactly out of phase. Recent hydrodynamic results also show that the bending locus is not characterized by increased flexibility[14].

Interruptions in the A tract

The importance of a continuous run of A residues for the bending phenomenon was investigated by interrupting the A_5 tract with another nucleotide N (sequence code IAN) at the central base. Figure 3 shows that these single base-pair changes cause the gel mobility to revert nearly to normal, from which we conclude that bending is almost abolished. Hence, a continuous run of A residues is the basis for the bending phenomenon; clearly, the purines A and G are not equivalent in this case.

The base least effective in interrupting the influence of a run of As is T; this observation may be of interest in considering possible DNA structural polymorphism in the TATA box region of promoters. In addition, we found that the sequence $(G_5N_5)_n$ has normal gel-electrophoretic mobility (data not shown), confirming the special role of A tracts (or T tracts if the complementary strand is examined).

Table 1 Sequences examined

Name	Sequence (5′ → 3′)
A_5N_4	C A A A A A C G G
A_5N_5	G G C A A A A A C G
A_5N_6	G G C C A A A A A C G
A_5N_7	G G C C A A A A A C C G
A_5N_{10}	C C G G C A A A A A C G G G C
IAC	G G C A A C A A C G
IAG	G G C A A G A A C G
IAT	G G C A A T A A C G
FCT	G G C A A A A A T G
FGG	C C G A A A A A G G
A_3N_7	G G C C A A A C C G
A_4N_6	G G C C A A A A C G
A_6N_4	G G C A A A A A A C
A_8N_2	C C A A A A A A A A
A_9N_1	C A A A A A A A A A
G_5N_5	T C G T G G G G C
A_{5-8}	C C A A A A A C G G G C A A A A A A A A
A_{8-5}	C C A A A A A A A A C G G G C A A A A A
A_6-T_6	A A A A C G G G T T T T T T G G G C A A
A_{20}	A A A A A A A A A A A A A A A A A A A A

Only one strand of each duplex is shown. All duplexes were constructed with 2-bp protruding 5′ ends, except A_5N_4, which had 1-bp protruding 5′ ends. Multimers of $dA_{20}\cdot dT_{20}$ were prepared both by ligation of the duplex and, for sequences 100, 140 and 160 bp long, by ligation of dA_{20} (or dT_{20}) on poly(dT) (or poly (dA)) followed by gel purification of the selected radiolabelled multimers and hybridization with the complementary strand of equal length. This procedure was followed because we could not be certain of the polarity of ligation of $dA_{20}\cdot dT_{20}$. A_5N_4, A_5N_5 and FGG were synthesized manually using the phosphotriester method and the remainder of the sequences were produced by automated DNA synthesis using phosphoramidite reagents on an Applied Biosystems instrument. A sequence A_7N_3 was synthesized, but since two multimeric ladders of differing gel mobilities were produced, depending on the conditions of ligation, those results are not reported here. Ligated multimers of A_5N_4 and A_5N_5 were cloned, and their sequence was verified by Maxam-Gilbert sequencing reactions.

Alterations in length of A tracts

To determine the influence of the length of the A tract, we synthesized the series $(A_jN_{10-j})_n$, in which the sequence phasing is kept constant at 10 bp, while the number of A residues in the continuous block is varied. The results collected in Fig. 3 show that an A tract of length 3 produces only slight electrophoretic anomalies; the effect is substantial with 4 As in a row, and increases to a maximum for a tract of length 6. Apparent bending is lessened but still substantial for $(A_8N_2)_n$ and $(A_9N_1)_n$. In

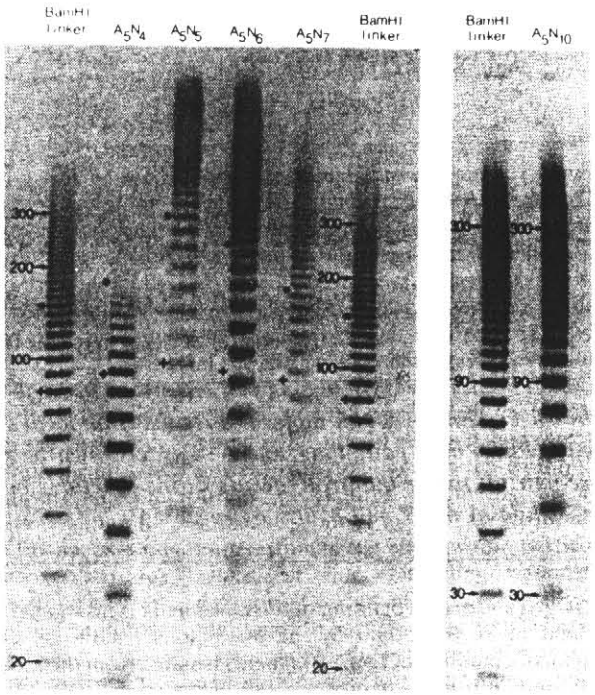

Fig. 1 Autoradiogram of the multimer series $(A_5N_k)_n$ ($k = 4, 5, 6, 7, 10$) electrophoresed on a non-denaturing 8% polyacrylamide gel. Mobility indicators, interpolated where necessary, are: +, multimers of 80-bp sequence length; *, 150-bp sequence length. Chemically synthesized oligonucleotides (Table 1) were purified on a 20% polyacrylamide gel, followed by high salt elution from a DE-52 ion-exchange column. Purified oligonucleotides were desalted using Sep-Pak C18 cartridges (Waters). 8 μg of each oligomer was 5′-labelled with 10 μCi of [γ-^{32}P]ATP (5 μCi pmol^{-1}; Amersham) in 10 μl of solution, at 37 °C for 15 min. The reaction solution contained 70 mM Tris-HCl (*p*H 7.6), 10 mM $MgCl_2$, 5 mM dithiothreitol (DTT) and 6 U polynucleotide kinase (New England Biolabs). After labelling with [γ-^{32}P]ATP, 50 nmol cold ATP and an additional 4 U of kinase were added, and the reaction volume was doubled to 20 μl. Kinasing with cold ATP was continued in the same buffer and temperature as above, for a period of 1 h. Two kinased oligonucleotides of complementary sequence (except for single-stranded residues at the 5′ ends) were mixed, heated to 55 °C and cooled slowly to 0 °C to form hybrids. To 10 μl of the hybridized mixture was added 800 U of T4 DNA ligase (New England Biolabs), and the reaction volume was adjusted to 20 μl; the ligation mixture had the same concentration of Tris-HCl, $MgCl_2$ and DTT as the kinasing step, plus 2.3 mM cold ATP. The ligation reaction was allowed to proceed on ice overnight, after which it was quenched by addition of EDTA (*p*H 8.0) to 25 mM final concentration. Ligated products were run on non-denaturing 8% polyacrylamide gels (mono:bis acrylamide ratio = 29:1; 90 mM Tris-borate, 2.5 mM EDTA, *p*H 8.3) until the bromophenol blue dye had migrated 22 cm. The applied voltage was 7 V cm^{-1}, and electrophoresis was carried out at room temperature. Multimers of the *Bam*HI linkers (10 bp, New England Biolabs) were also electrophoresed adjacent to a pBR322-*Hin*fI digest (data not shown) to confirm their normal gel mobility.

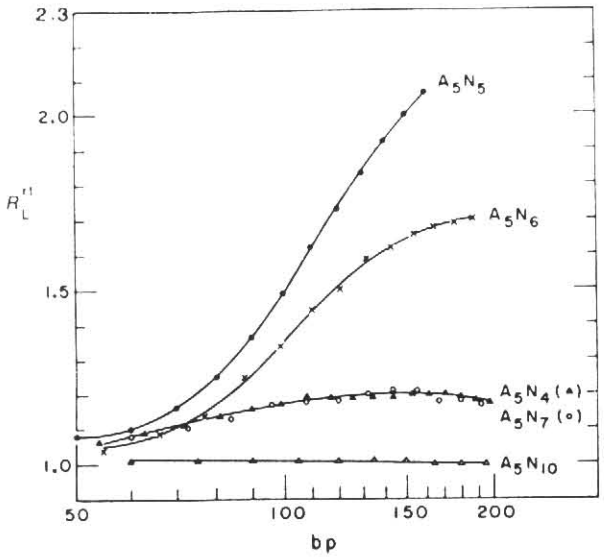

Fig. 2 The ratio R_L^{rt} (at room temperature) of apparent multimer size, determined from comparison with the electrophoresis markers, to actual chain length. Increasing R_L^{rt} indicates an anomalous structure which is interpreted as DNA bending. Strong anomalies are seen only when the sequence phasing of the A_5 tract is 10 (A_5N_5) or 11 (A_5N_6), corresponding to the number of base pairs in one double helical turn of DNA. Phasing of the A tracts at 1.5 helical turns (A_5N_{10}) produces no detectable bending, eliminating flexibility as an explanation for the phenomenon. Gels were run at room temperature.

order to be certain that the anomalous properties of these latter two sequences were not due to their high content of homopolymeric poly(dA)·poly(dT), we also examined the series $(A_{20})_n$, and found (Fig. 3) that these homopolymeric double helices have slightly increased electrophoretic mobility.

An interesting feature of the results in Fig. 3 is the crossover between the mobility curves for $(A_5N_5)_n$ and $(A_8N_2)_n$ at about 130 bp, with the latter showing greater mobility anomalies for molecules longer than the crossover size. We ascribe this behaviour to the strong influence of exact phasing on mobility anomalies: since $(A_8N_2)_n$ has the higher content of homopolymeric poly(dA·dT), its helix screw is more closely matched to the 10-bp sequence repeat characteristic of this series of molecules. A similar explanation can be applied to the crossover observed between the two series of polymeric A_4N_6 and A_9N_1 molecules.

Differential phasing of junctions

The substantial electrophoretic anomaly of $(A_9N_1)_n$ is surprising because the 3′ and 5′ ends of the A tract are nearly a full helical turn apart; if the junctions produced equivalent bends in opposite directions, as, for example, proposed for the junction of an A-DNA segment with B-DNA[15], one would expect the bends to compensate for each other when placed one helical turn apart. This observation raises the possibility that the bend is concentrated primarily at a single site, for which the only logical choices are the 3′ and 5′ junctions of the block of As. Therefore, we synthesized the series $A_{5\text{-}8}$ and $A_{8\text{-}5}$, which differ in that the former maintains a uniform 10-bp phasing of the 5′ ends of the A tracts, with an alternating 7- and 13-bp separation between the 3′ ends, whereas the latter has uniform 10-bp phasing of the 3′ ends, with the 5′ ends now characterized by the 7- and 13-bp alternating separation. Figure 3 shows that $A_{8\text{-}5}$ is clearly more anomalous, and hence more strongly bent, than $A_{5\text{-}8}$. We conclude that accurate phasing of the 3′ ends of the A tracts is a dominant factor in bending; it follows that a substantial portion of the bending is concentrated at the 3′ junction. However, the 5′ junction must also contribute, as bending is maximized when both 3′ and 5′ junctions have 10-bp phasing, and are approximately half a helical turn (6 bp) apart, as in $(A_6N_4)_n$.

We investigated the symmetry properties of the bending locus through synthesis of $(A_6\text{-}T_6)_n$, in which every other CA_6C element is inverted to GT_6G. These molecules, with $R_L[140\text{ bp}] = 2.13$, are nearly as anomalous as $(A_6N_4)_n$. We conclude that 2-fold rotation of an A_6 bending locus does not substantially alter the direction of bending.

Role of flanking bases

Given the importance of the junctions of the A tracts, it might be expected that the extent of bending would depend on the flanking bases. We found this to be the case, although the effects are not dramatic. Among the limited set of sequences examined, the greatest degree of bending ($R_L[150\text{ bp}] = 2.07$ for sequence FCT; see Table 1) is seen when the 5′-flanking base is C and the 3′ base is T, as found at the natural bending locus in *L. tarentolae*. The sequence with a flanking C both 3′ and 5′ is less bent ($R_L[150\text{ bp}] = 2.00$ for A_5N_5), and the phenomenon is reduced further ($R_L[150\text{ bp}] = 1.80$ for FGG) when G is present at both 3′ and 5′ ends.

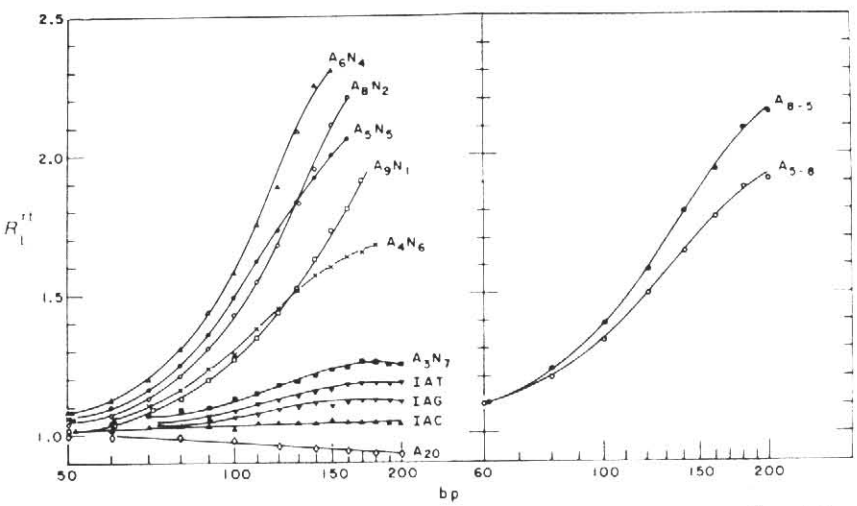

Fig. 3 *a*, R_L^{rt} (at room temperature) of multimers containing A tracts of different lengths, with constant sequence phasing. Values for the $(A_{20})_n$ series were obtained from the products of a ligation reaction carried out on $(dA)_{20}\cdot(dT)_{20}$ as described in Fig. 1 legend. In addition, the mobilities were checked against $(dA)_n\cdot(dT)_n$ (n = 100,140,160) because of uncertainty about the polarity of ligation of $(dA)_{20}\cdot(dT)_{20}$. We prepared $(dA)_n$ by kinasing A_{20}, hybridizing with an equal concentration (by absorbance at 260 nm) of poly(dT) (Sigma) as template, and ligating as described for Fig. 1 at 4 °C overnight. Ligated multimers of A_{20} were separated on an 8% denaturing polyacrylamide gel, and bands corresponding to the desired chain lengths were cut out, electroeluted, phenol-extracted and ethanol-precipitated. The corresponding $(dT)_n$ oligomers were prepared analogously, using poly(dA) as template, and hybridized with the $(dA)_n$ strand of equal length for gel analysis. *b*, R_L^{rt} (measured at room temperature) for the sequences $A_{5\text{-}8}$ and $A_{8\text{-}5}$, which differ in phasing of the 5′ and 3′ junctions. The difference in gel anomalies for the two sequences demonstrates non-equivalence of the 3′ and 5′ junctions; the greater anomaly in $A_{8\text{-}5}$, in which the 3′ junctions are phased at 10-bp intervals, implies greater bending at the 3′ than at the 5′ junction.

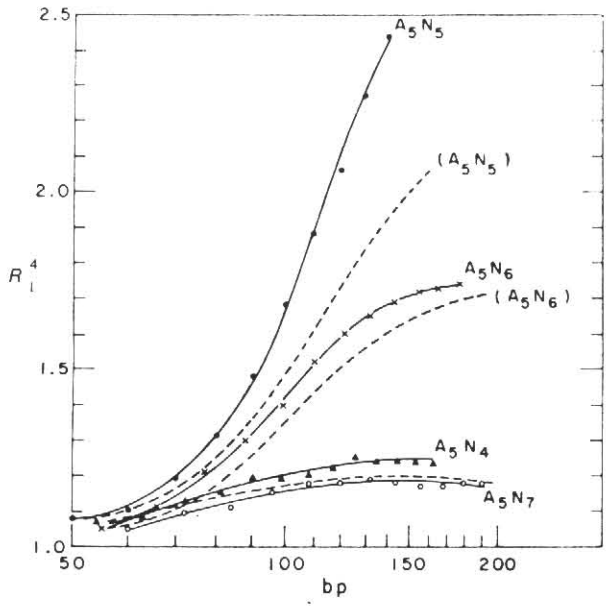

Fig. 4 Effect of lowered temperature on the gel mobility of the series $(A_5N_k)_n$, $n = 4,5,6,7$. R_L^4 values are shown for an 8% polyacrylamide gel, run at 4 °C, with voltage gradient 8 V cm^{-1}. The dashed lines show the results for gels run at room temperature (Fig. 2).

Temperature

It has been reported[4,16] that increased temperature causes the gel mobility of kinetoplast DNA fragments to revert to more normal values, a property we found also to be characteristic of synthetic bending sequences. Figure 4 compares apparent lengths measured from gels run at 4 °C and at room temperature for the series A_5N_k. Both of the highly anomalous series of molecules A_5N_5 and A_5N_6 become even more so at lower temperature, from which we conclude that bending is increased at lower temperature. However, the response of molecules longer than 100 bp is dramatically different in the two cases, implying a second effect in addition to an increase in the average bending angle; a possible explanation is the effect of lowered temperature on the DNA helical screw[17], as discussed below.

Figure 5*a*, *b* summarizes the influence of lowered temperature on mobility anomalies of the series $(A_jN_{10-j})_n$. The molecules $(A_4N_6)_n$ and $(A_5N_5)_n$ are most strongly affected by lowered temperature, to the extent that $(A_5N_5)_n$ becomes nearly as anomalous as $(A_6N_4)_n$, and retains greater anomaly than $(A_8N_2)_n$ even for molecules longer than 130 bp. Improved phasing match in $(A_5N_5)_n$ at 4 °C doubtless contributes to this trend. The very weak bending observed for $(A_3N_7)_n$ at room temperature increases at 4 °C, but remains much below that observed for other members of the series. Only $(A_9N_1)_n$ shows a general decline in the extent of mobility anomaly, for molecules between 60 and 150 bp in length, as temperature is decreased.

Models for DNA bending

We have identified two general classes of models for the origin of sequence-directed DNA bending: (1) models which assume that A tracts retain a normal B-DNA structure, and that bending can be explained in terms of nearest (or sometimes next-nearest) neighbour nucleotide sequences, and (2) models which invoke a longer-range structural polymorphism at the A tract, and which focus on the properties of junctions between it and adjacent B-DNA.

Class 1 includes the original analysis by Trifonov and colleagues[18,19] of sequence periodicities which were proposed to produce 'curving' of eukaryotic DNA and thus ease its packaging in chromatin. Their approach identified the dinucleotides ApA (and TpT) which are clearly related to the A-tract bending phenomenon. The Dickerson–Calladine[20–22] analysis of base-pair roll resulting from purine–purine clash also falls into this category, although because of compensating roll at sequences adjacent to a purine–pyrimidine (Pu–Py) dinucleotide, the Dickerson[22] parameters do not predict the bending observed in the kinetoplast DNA sequence[3]. On the other hand, the conformational analysis reported by Zhurkin and colleagues[23,24] predicts that Pu–Py sequences should favour bending by compressing the minor groove, whereas Py–Pu sequences should bend into the major groove. Clearly, this model would predict systematic bending in the kinetoplast sequence with its 5–6-bp alternation of Pu–Py and Py–Pu nearest neighbours.

Models of class 2 take as their starting point the observation that poly(dA)·poly(dT) has an anomalous structure, as revealed by fibre diffraction[25], its 10.1-bp helical screw[11–13], its Raman spectrum[26,27], and its inability to be reconstituted into nucleosomes[28,29]. Hence, it is possible that oligo(dA·dT) tracts in DNA can adopt one or more alternative structures in addition to the normal B configuration. One expects that the tendency to form the alternative structure will increase with the length of the A tract, because short runs of A do not gain enough free energy from the structural switch to compensate for the unfavourable free energy at the junctions with normal DNA. If the base pairs

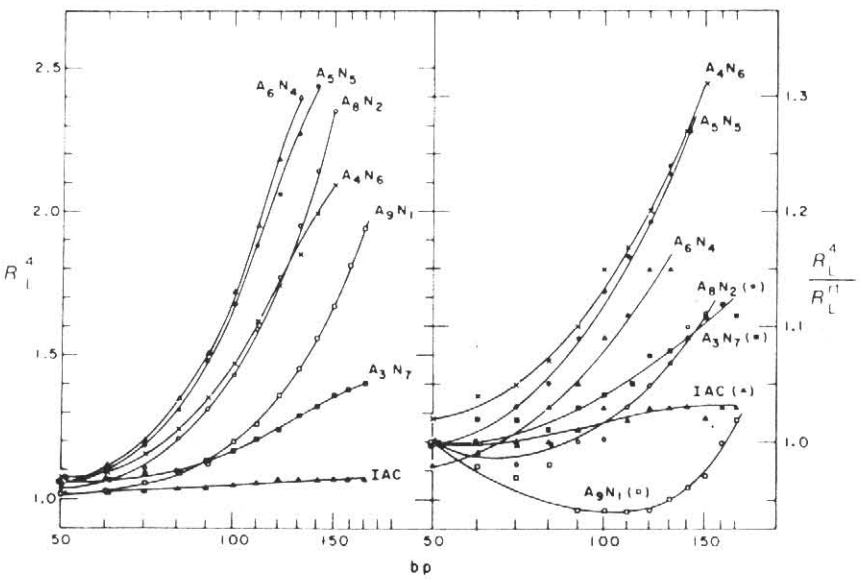

Fig. 5 Effect of lowered temperature on the mobility of the series $(A_jN_{10-j})_n$ and IAC (see Table 1), showing R_L^4 measured on a gel run at 4 °C as in Fig. 4. *b*, Relative changes in R_L values with temperature, shown as the ratio R_L^4/R_L^{rt}.

are tilted in the alternative structure, as proposed from fibre diffraction for the 'heteronomous'[25] (H) structure of poly(dA)·poly(dT), then a bend in the helix axis is expected at the junction with B-DNA, as illustrated by models built to represent the junction of A- and B-DNA[15]. Note that the two strands in the H-DNA model are not equivalent, so there is no necessity for the 3′ and 5′ junctions of H-DNA with B-DNA to exhibit the kind of equivalence required for A–B junctions by the 2-fold structural symmetry of A- and B-DNA.

Interpretation of the results

The general requirement, characteristic of all the models, for phasing the A tracts in coherence with the helical repeat is clearly verified by our experiments. When that finding is combined with the lack of bending found for molecules in which the phasing is 1.5 helical turns, we can definitely exclude increased flexibility from the list of possible explanations for the observed electrophoretic anomalies.

Our results clearly favour models of class 2, in which runs of A of sufficient length adopt an alternative helical structure. This readily explains the requirement of at least four successive A residues in order to observe strong bending anomalies. In addition, loss of the bending phenomenon when A_5 is replaced by AAGAA eliminates all models that are based on purine clash or preferential bending at Pu–Py and Py–Pu sequences. In the model which invokes bending at ApA dinucleotides, ApA bends separated by half a helical turn cancel each other. On that basis one would expect that the bending in $(A_3N_7)_n$ or in the IAN set, each of which has two putative ApA bending steps, should nearly equal the bending in $(A_9N_1)_n$, in which all but two of the ApA steps cancel. This prediction is definitely in disagreement with the facts. The essential problem with models of class 1 is that the bending observed in short A tracts is substantially less than expected. (We do not argue that small bends based on nearest-neighbour sequence do not occur, only that they cannot explain the A-tract bending phenomenon.)

The striking temperature dependence of bending is also readily explained in terms of the structural polymorphism model, by postulating that the equilibrium between B and the alternative structural form, provisionally called H, is shifted towards H at low temperature. This shift increases the average A-tract bending angle, and also affects the accuracy of helical phasing of the bending loci. Since junctions and therefore bends are absent when the A tract is in the B-form, higher temperature eliminates bending as the H-form disappears. Lowered temperature is expected to improve the phase match in $(A_5N_5)_n$ and $(A_4N_6)_n$ because conversion to the H-form brings the average helical screw closer to the 10-bp sequence repeat. In the case of $(A_5N_6)_n$, this factor works in the opposite direction because the helix is already overwound relative to the 11-bp sequence repeat, leaving only a modest increase in observed bending at low temperature, due to the increased average A-tract bending angle.

The unusual temperature dependence observed for A_9N_1 may result from a tendency of the H segment to include the single C residue, thus bridging continuously from one A tract to another. This would result in reduced average bending because H–B junctions would disappear, and would alter the otherwise expected increase of bending on lowering the temperature.

The observed non-equivalence in the importance of the 3′ and 5′ A-tract junctions for bending implies lack of 2-fold symmetry in the structure of the A tract. This supports the proposal that the structure may resemble H-DNA, whose most unusual feature is a lack of equivalence between the strands. A schematic model is shown in Fig. 6, based on the conformation of the dA strand in the H-form structure[25] and on the observation reported by Edmondson and Johnson[30] that T has a greater angle relative to the helix axis than does A in poly(dA)·poly(dT). It is a natural consequence of the model shown that bending is greater at the 3′ than at the 5′ junction of the A tract.

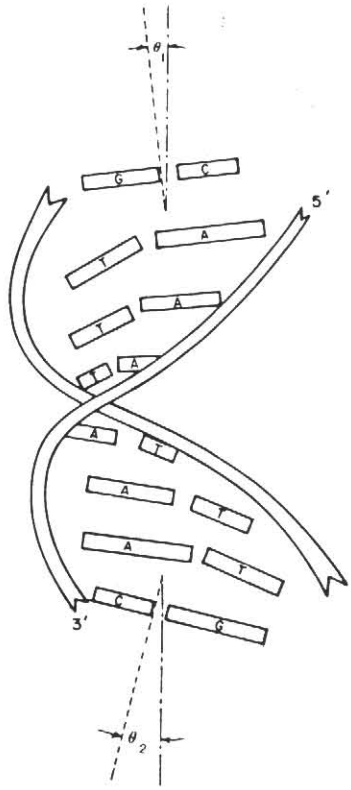

Fig. 6 Proposed model for differential bending at the 3′ and 5′ junctions. The A-tract helix backbone trajectories and tilt of the A residues are taken from the H-DNA structural model[25], and the extra tilt of the T residues is based on the optical experiments of Edmondson and Johnson[30]. (—·—, Helix axis of the A-tract segment, assumed to be in the H-form structure; - - -, helix axes of the adjacent B-DNA segments. At the 5′ junction, the G·C base pair from the top B-DNA segment stacks parallel to the A base, rather than the T base, because of the stronger stacking interactions of A. At the 3′ junction, the downward-tilted T residue prevents the G·C pair that begins the lower B-DNA segment from stacking parallel to the A base. As a consequence, the helix axis bending angle θ_2 is greater than the corresponding angle θ_1. The pseudo-2-fold axis for the CA_6C segment lies in the plane of the paper, and runs through the centre of the A_6 tract; rotation about that axis produces no change in predicted bending, as is nearly true for the sequence A_6-T_6. The model is intended to be schematic; the bending angles θ and the base tilt angles have only qualitative significance.

The model in Fig. 6 also explains the observation that 2-fold rotation of every other CA_6C bending locus has little effect on the extent of bending. The pseudo-dyad axis in the model lies in the plane of the paper, and runs between the third and fourth A in the tract. The total bending in the direction of base-pair tilt at the two junctions as shown is not affected by rotation about the approximate 2-fold axis. However, if bending were in the direction of base-pair roll into the major groove at one junction and into the minor groove at the other (in a direction perpendicular to the paper in the model), 2-fold rotation would invert the direction of bending, and the effects of successive A and T tracts would cancel. Hence, models which rely on base-pair roll at H–B junctions can be eliminated.

Our results lead us to stress the potential general importance of local polymorphism of DNA structure. In the case of A-tract bending, a cooperatively induced, altered helical structure is clearly implied, with special effects at the 3′ junction of the A tract with adjacent B-DNA. The recent observation by Reynolds *et al.*[31] of specific antibiotic-induced cleavage at the 3′ end of A tracts supports the view that DNA structure is significantly altered at that site. In addition, their observation that the same

drug cuts in the promoter TATA box suggests that a similar alteration may be possible there. Such structural variations may have wide significance for protein–DNA recognition.

This work was supported by NSF grant DMB-8405494 and by a Project Grant for Parasitology and Tropical Medicine from the MacArthur Foundation. The DNA synthesizer was purchased with the help of NSF grant PCM 8413761. We thank Sarah Woodson and Aino Ruusala for advice and assistance with oligonucleotide synthesis, and Abraham Brown for discussions and for bringing ref. 31 to our attention.

Received 6 December 1985; accepted 4 March 1986.

1. Englund, P. T., Hajduk, S. L. & Marini, J. C. *A. Rev. Biochem.* **51**, 695–726 (1982).
2. Marini, J. C., Levene, S. D., Crothers, D. M. & Englund, P. T. *Proc. natn. Acad. Sci. U.S.A.* **79**, 7664–7668 (1982).
3. Levene, S. D. & Crothers, D. M. *J. biomolec. Struct. Dyn.* **1**, 429–435 (1983).
4. Marini, J. C. *et al. J. biol. Chem.* **259**, 8974–8979 (1984).
5. Ntambi, J. M. *et al. Molec. Biochem. Parasit.* **12**, 273–286 (1984).
6. Wu, H. M. & Crothers, D. M. *Nature* **308**, 509–513 (1984).
7. Hagerman, P. J. *Proc. natn. Acad. Sci. U.S.A.* **81**, 4632–4636 (1984).
8. Zahn, K. & Blattner, F. R. *Nature* **317**, 451–453 (1985).
9. Lerman, L. S. & Frisch, H. L. *Biopolymers* **21**, 995–997 (1982).
10. Lumpkin, O. J. & Zimm, B. H. *Biopolymers* **21**, 2315–2316 (1982).
11. Peck, L. C. & Wang, J. C. *Nature* **292**, 375–378 (1981).
12. Rhodes, D. & Klug, A. *Nature* **292**, 378–380 (1981).
13. Strauss, F., Gaillard, C. & Prunell, A. *Eur. J. Biochem.* **118**, 215–222 (1981).
14. Levene, S. D., Wu, H. M. & Crothers, D. M. *Biochemistry* (in the press).
15. Selsing, E., Wells, R. D., Alden, C. J. & Arnott, S. *J. biol. Chem.* **254**, 5417–5422 (1979).
16. Wu, H. M. thesis, Yale Univ. (1982).
17. Depew, R. E. & Wang, J. C. *Proc. natn. Acad. Sci. U.S.A.* **72**, 4275–4279 (1975).
18. Trifonov, E. N. & Sussman, J. L. *Proc. natn. Acad. Sci. U.S.A.* **77**, 3816–3820 (1980).
19. Trifonov, E. N. *Nucleic Acids Res.* **8**, 4041–4053 (1980).
20. Drew, H. R. *et al. Proc. natn. Acad. Sci. U.S.A.* **78**, 2179–2183 (1981).
21. Calladine, C. R. *J. molec. Biol.* **161**, 343–352 (1982).
22. Dickerson, R. E. *J. molec. Biol.* **166**, 419–441 (1983).
23. Zhurkin, V. B., Lysov, Y. P. & Ivanov, V. I. *Nucleic Acids Res.* **6**, 1081–1096 (1979).
24. Zhurkin, V. B. *J. biomolec. Struct. Dyn.* **2**, 785–804 (1985).
25. Arnott, S., Chandrasekaran, R., Hall, I. H. & Puigjaner, L. C. *Nucleic Acids Res.* **11**, 4141–4155 (1983).
26. Thomas, G. A. & Peticolas, W. L. *J. Am. chem. Soc.* **105**, 993–996 (1983).
27. Jolles, B., Laigle, A., Chinsky, L. & Turpin, P. Y. *Nucleic Acids Res.* **13**, 2075–2085 (1985).
28. Simpson, R. T. & Kunzler, P. *Nucleic Acids Res.* **6**, 1387–1415 (1979).
29. Kunkel, G. R. & Martinson, H. G. *Nucleic Acids Res.* **9**, 6869–6888 (1981).
30. Edmondson, S. P. & Johnson, W. C. Jr *Biopolymers* **24**, 825–841 (1985).
31. Reynolds, V. L., Molineux, I. J., Kaplan, D. J., Swenson, D. H. & Hurley, L. H. *Biochemistry* **24**, 6228–6237 (1985).

Large-scale anisotropy in the Hubble flow

C. A. Collins*, R. D. Joseph & N. A. Robertson*

Blackett Laboratory, Imperial College, London SW7 2BZ, UK

Detection of anisotropy in the Hubble flow is one of the outstanding problems of observational cosmology. It provides information on the mass density of the Universe and the extent to which the Universe is smooth. This, in turn, permits constraints to be placed on theoretical models of galaxy formation. Our approach to this problem has been to obtain infrared photometry for an all-sky sample of ScI-II galaxies identified by Rubin *et al.*[1] at a mean redshift of 5,100 km s^{-1}. At this distance these galaxies provide information on the Hubble flow well outside the Local Supercluster. From observations of half the sample, well distributed across the sky, we find a systematic streaming velocity of these galaxies of ~1,000 ± 300 km s^{-1}. In the context of current speculation regarding non-baryonic particle species which may dominate the mass of the Universe, such large velocities on these spatial scales appear to exclude cold dark matter models.

We have used infrared photometry to measure the distances to this all-sky sample of galaxies. Infrared magnitudes have the advantage of being relatively unaffected by extinction and provide a reliable indication of distance when combined with either the optical–infrared colour–magnitude relation[2] or the infrared Tully–Fisher relation[3]. We have measured 45 of the 96 ScI-II galaxies comprising the Rubin *et al.*[1] 'minimum bias subset' in the J, H and K wavelength bands with a 35 arc s aperture using the 1.5-m Infrared Flux Collector in Tenerife. These 45 galaxies are well distributed across the sky (see Fig. 1). In particular, their redshift distribution is representative of that for the entire sample.

Our approach is to search for a systematic dipole velocity by comparing the velocities inferred from photometry with the observed recessional velocities. The analysis is carried out to find an apparent Local Group motion relative to the galaxy sample. Using the measured H magnitudes and the redshifts tabulated by Rubin *et al.*[1], we have carried out three different solutions for the apparent Local Group motion. For the first solution the H magnitudes were corrected for Malmquist bias in the sample and for the effect of using a fixed aperture. Both

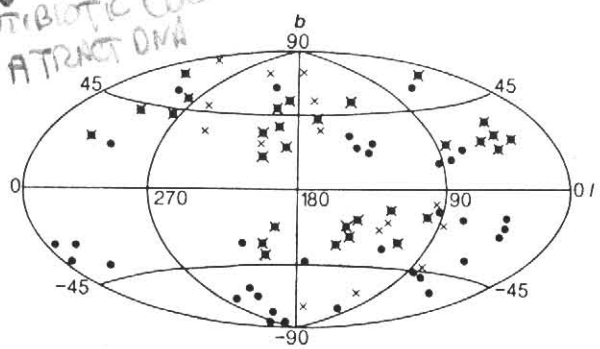

Fig. 1 Positions of galaxies observed in galactic coordinates on an equal-area projection of the celestial sphere. ×, Galaxies observed in bands J, H and K; ●, galaxies detected by IRAS.

of these effects result in an apparent increase of galaxy luminosity with redshift. A 'composite' correction for these effects was determined from a plot of Hubble modulus (defined below) versus redshift. Hubble velocities were then derived from the corrected H magnitudes, assuming all the galaxies have the same absolute magnitude. Following the Rubin *et al.*[4] approach, one need make no assumption about the precise value of the Hubble constant, H_0, or the absolute magnitude, M, of the sample. Instead one uses the Hubble modulus, HM, defined as

$$\mathrm{HM} = \log_{10} H_0 - 0.2\,M - 5 = \log_{10} v_{\mathrm{obs}} - 0.2\,m$$

where v_{obs} and m are the redshift and apparent magnitude of a galaxy. The mean HM for the sample can then be used to find the Hubble velocity for each galaxy, assuming uniform expansion, from

$$v_{\mathrm{H}} = 10^{(<HM>+0.2\,m)}$$

The difference between the observed redshift and the derived Hubble velocity, $v_{\mathrm{obs}} - v_{\mathrm{H}}$, and a putative systematic dipole velocity, v_{D}, are minimized in the least-squares sense, to derive a value for v_{D}. Because the redshifts have been corrected for the solar motion with respect to the Local Group (300 km s^{-1} toward galactic longitude $l = 90°$, latitude $b = 0°$), v_{D} is the velocity of the Local Group relative to the frame defined by these galaxies. The result is shown in the first line of Table 1. Identical results, within the errors, are obtained using the J and K magnitudes.

In our second solution we used the H I 21-cm velocity widths and the infrared Tully–Fisher relation[3] to find the relative lumi-

* Present addresses: Department of Astronomy, University of Edinburgh, Edinburgh EH9 3HJ, UK (C.A.C.) and Department of Natural Philosophy, Glasgow University, Glasgow G12 8QQ, UK (N.A.R.)